

# Beyond In-Domain Scenarios: Robust Density-Aware Calibration

Christian Tomani<sup>\*1</sup>, Futa Waseda<sup>\*2</sup>, Yuesong Shen<sup>1</sup>, Daniel Cremers<sup>1</sup>

<sup>1</sup>Technical University of Munich, <sup>2</sup>The University of Tokyo

{christian.tomani, yuesong.shen, cremers}@tum.de, futa-waseda@g.ecc.u-tokyo.ac.jp

## Abstract

Calibrating deep learning models to yield uncertainty-aware predictions is crucial as deep neural networks get increasingly deployed in safety-critical applications. While existing post-hoc calibration methods achieve impressive results on in-domain test datasets, they are limited by their inability to yield reliable uncertainty estimates in domain-shift and out-of-domain (OOD) scenarios. We aim to bridge this gap by proposing **DAC**, an accuracy-preserving as well as **Density-Aware Calibration** method based on k-nearest-neighbors (KNN). In contrast to existing post-hoc methods, we utilize hidden layers of classifiers as a source for uncertainty-related information and study their importance. We show that DAC is a generic method that can readily be combined with state-of-the-art post-hoc methods. DAC boosts the robustness of calibration performance in domain-shift and OOD, while maintaining excellent in-domain predictive uncertainty estimates. We demonstrate that DAC leads to consistently better calibration across a large number of model architectures, datasets, and metrics. Additionally, we show that DAC improves calibration substantially on recent large-scale neural networks pre-trained on vast amounts of data.

## 1 Introduction

Deep learning models have become state-of-the-art (SOTA) in several different fields. Especially in safety-critical applications such as medical diagnosis and autonomous driving with changing environments over

<sup>\*</sup>These authors contributed equally to this work

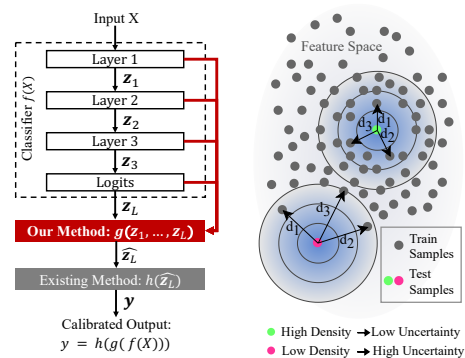


Figure 1: **Left:** Our density-aware calibration method (DAC)  $g$  can be combined with existing post-hoc methods  $h$  leading to robust and reliable uncertainty estimates. To this end, DAC leverages information from feature vectors  $z_1 \dots z_L$  across the entire classifier  $f$ . **Right:** DAC is based on KNN, where predictive uncertainty is expected to be high for test samples lying in low-density regions of the empirical training distribution and vice versa.

time, reliable model estimates for predictive uncertainty are crucial. Thus, models are required to be accurate as well as calibrated, meaning that their predictive uncertainty (or confidence) matches the expected accuracy. Due to the fact that many deep neural networks are generally uncalibrated [8], post-hoc calibration of already trained neural networks has received increasing attention in the last few years.

In order to tackle the miss-calibration of neural networks, researchers have come up with a plethora of post-hoc calibration methods [8, 47, 30, 23, 36, 9]. These current approaches are particularly designed for in-domain calibration, where test samples are drawn from the same distribution as the network was trained on. Although these approaches perform almost perfect in-domain, recent works [37] have shown that they lack substantially in providing reliable confidence scores

in domain-shift and out-of-domain (OOD) scenarios (up to 1 order of magnitude worse than in-domain), which is unacceptable, particularly in safety-critical real-world scenarios where calibration of neural networks matters in order to prevent unforeseeable failures. To date, the only post-hoc methods that have been introduced to mitigate this shortcoming in domain-shift and OOD settings, use artificially created data or data from different sources in order to estimate the potential test distribution [37, 43, 38]. However, these methods are not generic in that they require domain knowledge about the dataset and might only work well for a subset of anticipated distributional shifts, because they rely heavily on strong assumptions towards the potential test distribution. Furthermore, they can hurt in-domain calibration performance.

To mitigate the issue of miss-calibration in scenarios where test samples are not necessarily drawn from dense regions of the empirical training distribution or are even OOD, we introduce a density-aware method that extends the field of post-hoc calibration beyond in-domain calibration. Contrary to the aforementioned existing works which focus on particularly crafted training data, our method DAC does not depend on additional data and does not rely on any assumptions about potentially shifted or out-of-domain test distributions, and is even domain agnostic. The proposed method can, therefore, simply be added to an existing post-hoc calibration pipeline, because it relies on the exact same training paradigm with a held-out in-domain validation set as current post-hoc methods do.

Previous works on calibration have focused primarily on post-hoc methods that solely take softmax outputs or logits into account [8, 47, 30, 23, 36, 9]. However, we argue that prior layers in neural networks contain valuable information for recalibration too. Moreover, we report, which layers our method identified as particularly relevant for providing well-calibrated predictive uncertainty estimates.

Recently developed large-scale neural networks that benefit from pre-training on vast amounts of data [16, 22], have mostly been overlooked when benchmarking post-hoc calibration methods. One explanation for that could be because, e.g., vision transformers (ViTs) [5] are well calibrated out of the box [24]. Nevertheless, we show that also these models can profit from post-hoc methods and in particular from DAC through more robust uncertainty estimates.

## 1.1 Contribution

- We propose DAC, an accuracy-preserving and density-aware calibration method that can be combined with existing post-hoc methods to

boost domain-shift and out-of-domain performance while maintaining in-domain calibration.

- We discover that the common practice of using solely the final logits for post-hoc calibration is sub-optimal and that aggregating intermediate outputs yields improved results.
- We study recent large-scale models, such as transformers, pre-trained on vast amounts of data and encounter that also for these models our proposed method yields substantial calibration gains.

## 2 Related Work

Calibration methods can be divided into post-hoc calibration methods and methods that adapt the training procedure of the classifier itself. The latter one includes methods such as self-supervised learning [14], Bayesian neural networks [7, 40], Deep Ensembles [19], label smoothing [25] or mixup techniques [34, 46] as well as other intrinsically calibrated approaches [31, 35, 1]. Similar to post-hoc methods, Ovadia et al. [27] have found that intrinsic methods suffer as well from miss-calibration in domain-shift scenarios.

Post-hoc calibration methods, on the other hand, can be applied on top of already trained classifiers and do not require any retraining of the underlying neural network. Wang et al. [39] argue in favour of a unified framework comprising of main training and post-hoc calibration. Rahimi et al. [29] provide a theoretical basis for post-hoc calibration schemes in that learning calibration functions post-hoc using a proper loss function leads to calibrated outputs.

These post-hoc calibration methods include non-parametric approaches such as histogram binning [44], where uncalibrated confidence scores are partitioned into bins and are assigned a respective calibrated score via optimizing a bin-wise squared loss on a validation set. Isotonic regression [45], which is an extension to histogram binning, fits a piecewise constant function to intervals of uncalibrated confidence scores and Bayesian Binning into Quantiles (BBQ) [26] is different from isotonic regression in that it considers multiple binning models and their combination. In addition, Zhang et al. [47] introduce an accuracy-preserving version of isotonic regression beyond binary tasks, which they call multi-class isotonic regression (IRM). Moreover, Wenger et al. [41] and Milios et al. [23] propose Gaussian processes-based calibration methods.

Approaches for training a mapping function include Platt scaling [28], matrix as well as vector scaling and temperature scaling [8]. Temperature scaling (TS) transforms logits by a single scalar parameter in an accuracy-preserving manner, since re-scaling does not affect the

ranking of the logits. Moreover, Ensemble Temperature scaling (ETS) [47] extends temperature scaling by two additional calibration maps with a fixed temperature of 1 and  $\infty$ , respectively. More recent and advanced approaches include Dirichlet-based scaling [18] and Parameterized Temperature scaling [36], where a temperature is calculated sample-wise via a neural network architecture. Rahimi et al. [30] designed a post-hoc neural network architecture for transforming classifier logits that represent a class of intra-order-preserving functions, and Gupta et al. [9] introduce a method for obtaining a calibration function by approximating the empirical cumulative distribution of output probabilities with the help of splines.

These post-hoc calibration methods are trained on a hold-out calibration set. Although there has been a surge of research on these approaches in recent years, Tomani et al. [37] have discovered that post-hoc calibration methods yield highly over-confident predictions under domain-shift and are, therefore, not well suited for OOD scenarios. They introduce a strategy where samples are perturbed in the calibration set before performing the post-hoc calibration step. However, such an approach makes a strong distributional assumption on potential domain-shifts during testing by perturbing training samples in a particular way, which may not necessarily hold in each case. To date, post-hoc calibration methods that are themselves capable of distinguishing in-domain samples from gradually shifted or out-of-domain samples without any distributional assumptions have not yet been addressed.

### 3 Method

#### 3.1 Definitions

We study the multi-class classification problem, where  $X \in \mathbb{R}^D$  denotes a  $D$ -dimensional random input variable and  $Y \in \{1, 2, \dots, C\}$  denotes the label with  $C$  classes with a ground truth joint distribution  $\pi(X, Y) = \pi(Y|X)\pi(X)$ . The dataset  $\mathbb{D}$  contains  $N$  i.i.d. samples  $\mathbb{D} = \{(X_n, Y_n)\}_{n=1}^N$  drawn from  $\pi(X, Y)$ .

Let the output of a trained neural network classifier  $f$  be  $f(X) = (y, \mathbf{z}_L)$ , where  $y$  denotes the predicted class and  $\mathbf{z}_L$  the associated logits vector. The softmax function  $\sigma_{SM}$  as  $p = \max_c \sigma_{SM}(\mathbf{z}_L)^{(c)}$  is then needed to transform  $\mathbf{z}_L$  into a confidence score or predictive uncertainty  $p$  w.r.t  $y$ . In this paper, we propose an approach to improve the quality of the predictive uncertainty  $p$  by recalibrating the logits  $\mathbf{z}_L$  from  $f(X)$  via a combination of two calibration methods:

$$p = h(g(f(X))) \quad (1)$$

where  $g$  denotes our density-aware calibration method

DAC rescaling logits for boosting domain-shift and OOD calibration performance and  $h$  denotes an existing state-of-the-art in-domain post-hoc calibration method (Fig. 1).

Following Guo et al. [8], perfect calibration is defined such that confidence and accuracy match for all confidence levels:

$$\mathbb{P}(Y = y|P = p) = P, \quad \forall P \in [0, 1] \quad (2)$$

Consequently, miss-calibration is defined as the difference in expectation between accuracy and confidence.

$$\mathbb{E}_P [|\mathbb{P}(Y = y|P = p) - P|] \quad (3)$$

#### 3.2 Measuring calibration

The expected calibration error (ECE) [26] is frequently used for quantifying miss-calibration. ECE is a scalar summary measure estimating miss-calibration by approximating equation (3) as follows. In the first step, confidence scores  $\hat{\mathcal{P}}$  of all samples are partitioned into  $M$  equally sized bins of size  $1/M$ , and secondly, for each bin  $B_m$  the respective mean confidence and the accuracy is computed based on the ground truth class  $y$ . Finally, the ECE is estimated by calculating the mean difference between confidence and accuracy over all bins:

$$\text{ECE}^d = \sum_{m=1}^M \frac{|B_m|}{N} \|\text{acc}(B_m) - \text{conf}(B_m)\|_d \quad (4)$$

with  $d$  usually set to 1 (L1-norm).

#### 3.3 Density-Aware Calibration (DAC)

Our main idea for our proposed calibration method  $g$  stems from the fact that test samples lying in high-density regions of the empirical training distribution can generally be predicted with higher confidence than samples lying in low-density regions. For the latter case, the network has seen very few, if any, training samples in the neighborhood of the respective test sample in feature space, and is thus not able to provide reliable predictions for those samples. Leveraging this information about density through a proxy can result in better calibration.

In order to estimate such a proxy for each sample, we propose to utilize non-parametric density estimation using k-nearest-neighbor (KNN) based on feature embeddings extracted from the classifier. KNN has successfully been applied in out-of-distribution detection [33]. In contrast to Sun et al. [33], who only take the penultimate layer into account, we argue that prior layers yield important information too, and therefore,

incorporate them in our method as follows. We call our method Density-Aware Calibration (DAC).

Temperature scaling [8] is a frequently used calibration method, where a single scalar parameter  $T$  is used to re-scale the logits of an already trained classifier in order to obtain calibrated probability estimates  $\hat{Q}$  for logits  $\mathbf{z}_L$  using the softmax function  $\sigma_{SM}$  as

$$\hat{Q} = \sigma_{SM}(\mathbf{z}_L/T) \quad (5)$$

Similar to temperature scaling, our method is also accuracy preserving, in that we use one parameter  $S(\mathbf{x}, w)$  for re-scaling the logits of the classifier:

$$\hat{Q}(\mathbf{x}, w) = \sigma_{SM}(\mathbf{z}_L/S(\mathbf{x}, w)) \quad (6)$$

In contrast to temperature scaling, in our case,  $S(\mathbf{x}, w)$  is sample-dependent with respect to  $\mathbf{x}$  and is calculated via a linear combination of density estimates  $s_l$  as follows:

$$S(\mathbf{x}, w) = \sum_{l=1}^L w_l s_l + w_0 \quad (7)$$

with  $w_1 \dots w_L$  being the weights for every layer in  $L$  and  $w_0$  being a bias term. Note that only positive weights are valid because negative weights would assign high confidence to outliers. Thus, we constrain the weights to be positive to tackle overfitting.

For each feature layer  $l$ , we compute the density estimate  $s_l$  in the neighborhood of the empirical training distribution of the respective test sample  $\mathbf{x}$  with the  $k$ -th nearest neighbor distance: First, we derive the test feature vector  $\mathbf{z}_l$  from the trained classifier  $f$  given the test input sample  $\mathbf{x}$  and average over spatial dimensions as well as normalize it. We then use the normalized training feature vectors  $Z_{N_{Tr},l} = (\mathbf{z}_{1,l}, \mathbf{z}_{2,l}, \dots, \mathbf{z}_{N_{Tr},l})$ , which we gathered from the training dataset  $X_{N_{Tr}} = (\mathbf{x}_1, \mathbf{x}_2, \dots, \mathbf{x}_{N_{Tr}})$  to calculate the euclidean distance between  $\mathbf{z}_l$  and each element in  $Z_{N_{Tr},l}$  for each sample  $i$  in the training set  $N_{Tr}$  as follows:

$$d_{i,l} = \|\mathbf{z}_{i,l} - \mathbf{z}_l\| \quad (8)$$

The resulting sequence  $D_{N_{Tr},L} = (d_{1,l}, d_{2,l}, \dots, d_{N_{Tr},l})$  is reordered. Finally,  $s_l$  is given by the  $k$ -th smallest element ( $=k$ -th nearest neighbor) in the sequence:  $s_l = d_{(k)}$ , with  $(k)$  indicating the index in the reordered sequence  $D_{N_{Tr},L}$ . For determining  $k$ , we follow Sun et al. [33], who did a thorough analysis and concluded that a proper choice for  $k$  is 50 for CIFAR10, 200 for CIFAR100 for all training samples and 10 for ImageNet for 1% training samples.

We fit our method for a trained neural network  $f(X) = (y, \mathbf{z}_L)$  by optimizing a squared error loss  $L_w$  w.r.t.  $w$ .

$$L_w = \sum_{c=1}^C (I_c - \sigma_{SM}(\mathbf{z}_L/S(\mathbf{x}, w))^{(c)})^2 \quad (9)$$

where  $I_c$  indicates a binary variable, which is 1 if the respective sample has true class  $c$ , and 0 otherwise. We accumulate  $L_w$  over all samples in the validation set.

The rescaled logits  $\hat{\mathbf{z}}_L(\mathbf{x}, w) = \mathbf{z}_L/S(\mathbf{x}, w)$  and consequently the recalibrated probability estimates  $\hat{Q}(\mathbf{x}, w)$  can directly be fed to another post-hoc method. Thus, DAC can be applied prior to other existing in-domain post-hoc calibration methods for robustly calibrating models in domain-shift and OOD scenarios (Fig. 1).

Our method has the following advantages:

- **Density aware:** Due to distance-based density estimation across feature layers, our method is capable of inferring how close or how far a test sample is in feature space with respect to the training distribution and can adjust the predictive estimates of the classifier accordingly.
- **Domain agnostic:** Since we use KNN, a non-parametric method for density estimation, no distributional assumptions are imposed on the feature space, and our method is therefore applicable to any type of in-domain, domain-shift, or OOD scenario.
- **Backbone agnostic:** Adapts easily to different underlying classifier architectures (e.g., CNNs, ResNets, and more recent models like transformers) because during training, DAC automatically figures out the informative feature layers regarding uncertainty calibration.

## 4 Experimental Setup

**Models and Datasets** In our study, we quantify the performance of our proposed model for various model architectures and different datasets. We consider 3 different datasets to evaluate our models on: CIFAR10/100 [17], and ImageNet-1k [4]. In particular, for measuring performance on CIFAR10 and CIFAR100, we train ResNet18 [10], VGG16 [32] and DenseNet121 [15], and for ImageNet, we use 3 pre-trained models, namely ResNet152 [10], DenseNet169 [15], and Xception[3]. We further investigate post-hoc calibration methods applied to new state-of-the-art architectures as well as modern training schemes. To this end, we include the following models in our study, which are all finetuned on ImageNet-1k:

- **BiT-M** [16]: Is a ResNet-based architecture (ResNetV2) [11] pre-trained on ImageNet-21k.
- **ResNeXt-WSL** [22]: Is a ResNeXt-based architecture (ResNeXt101 32x8d) [42], which is weakly

Table 1: Mean expected calibration error across all test domain-shift scenarios. For each model, the macro-averaged ECE ( $\times 10^2$ ) (with equal-width binning and 15 bins) is computed across all corruptions from severity=0 (in-domain) until severity=5 (heavily corrupted). Post-hoc calibration methods paired with our method are consistently better calibrated than simple post-hoc methods. (lower ECE is better)

	Uncal -	Baseline Calibration Methods					Combination with DAC (Ours)				
		TS	ETS	IRM	DIA	SPL	TS	ETS	IRM	DIA	SPL
C10 ResNet18	19.27	4.96	4.96	5.93	6.39	6.27	<u>4.49</u>	<b>4.39</b>	4.90	4.61	4.74
C10 VGG16	19.05	6.25	6.30	7.45	9.82	7.57	<b>5.66</b>	<b>5.66</b>	6.30	6.33	5.69
C10 DenseNet121	19.26	5.21	5.21	6.66	7.81	6.60	<u>4.59</u>	<u>4.59</u>	5.69	6.60	<b>4.42</b>
C100 ResNet18	16.44	11.37	10.56	12.26	9.24	10.40	10.66	<u>8.96</u>	10.04	<b>8.47</b>	9.74
C100 VGG16	34.41	11.54	11.54	13.24	14.62	10.76	<u>6.49</u>	<b>6.48</b>	8.11	10.26	7.45
C100 DenseNet121	23.83	8.80	<u>8.76</u>	12.07	11.02	9.73	8.77	<b>8.40</b>	10.05	15.01	9.15
IMG ResNet152	10.50	4.47	4.01	5.20	7.17	5.56	<u>3.48</u>	<b>3.34</b>	3.50	3.64	3.63
IMG DenseNet169	13.28	6.59	6.34	7.37	8.44	7.12	4.81	<b>3.87</b>	4.53	6.31	4.60
IMG Xception	30.49	8.81	8.40	12.93	9.83	10.80	8.79	<b>7.99</b>	<u>8.38</u>	8.99	8.49
IMG BiT-M	11.71	7.17	6.56	6.93	7.45	6.62	4.40	<u>3.98</u>	4.21	5.51	<b>3.76</b>
IMG ResNeXt-WSL	15.44	8.03	8.03	8.04	8.32	6.16	7.32	<u>5.63</u>	5.75	6.32	<b>3.90</b>
IMG ViT-B	3.78	4.23	3.72	4.24	5.85	3.93	3.80	<b>3.34</b>	3.99	5.52	<u>3.56</u>

supervised pre-trained with billions of hashtags of social media images.

- **ViT-B** [6]: Is a transformer-based architecture pre-trained on ImageNet-21k.

We quantify calibration performance for in-domain, domain-shift, and OOD scenarios. In order to ensure a gradual domain-shift in our evaluation pipeline, we use ImageNet-C as well as CIFAR-C [12], which were specifically developed to produce domain-shift and were incorporated in many related studies since. Both datasets have 18 distinct corruption types, each having 5 different levels of severity, mimicking a scenario where the input data to a classifier gradually shifts away from the training distribution. Additionally, we test our models on a real-world OOD dataset, namely ObjectNet-OOD. ObjectNet [2] is a dataset consisting of 50,000 test images with a total of 313 classes, of which 200 classes are out-of-domain with respect to ImageNet. Hence, we make use of these 200 classes for our OOD analysis.

**Post-hoc Calibration Methods** We consider the currently best performing post-hoc calibration methods for benchmarking as well as for combining them with DAC: Temperature scaling (TS) [8], Ensemble Temperature scaling (ETS) [47], accuracy preserving version of Isotonic Regression (IRM) [47], Intra-order preserving calibration (DIA) [30], Calibration using Splines (SPL) [9]. Additionally, we show results for Isotonic Regression (IR) [45], Parameterized Temperature scaling (PTS) [36] and Dirichlet calibration (DIR) [18].

Our proposed method DAC does not solely rely on

logits for calibration as other post-hoc calibration approaches do, it rather takes various layers at certain positions of the network into account. Even though DAC would be capable of using every layer in a classifier due to its weighting scheme, we opt for a much simpler and faster version. That is, we follow a structured approach for choosing layers, e.g., after each ResNet or transformer block. In the results, we show that our selective approach produces similar results compared to taking all layers into account.

**Measuring Calibration** Our evaluation is based on various calibration measures. Throughout the paper, we provide results for ECE using equal-width binning with 15 bins. Although ECE is the most commonly used metric for evaluating and comparing post-hoc calibration methods, it bears several limitations. That is why, in Appendix, we show that our results hold for different kinds of calibration measures, including ECE based on kernel density estimation (ECE-KDE) [47], ECE using equal-mass binning and class-wise ECE[18] as well as we demonstrate consistency with likelihood and Brier score.

## 5 Results

First, we show that combining our method DAC with existing post-hoc calibration methods increases calibration performance across the entire spectrum, from in-domain to heavily corrupted data distributions, for different datasets and various model architectures, including transformers. Secondly, we show the calibration performance of our method on purely OOD scenarios. Lastly, we conduct additional experiments, such

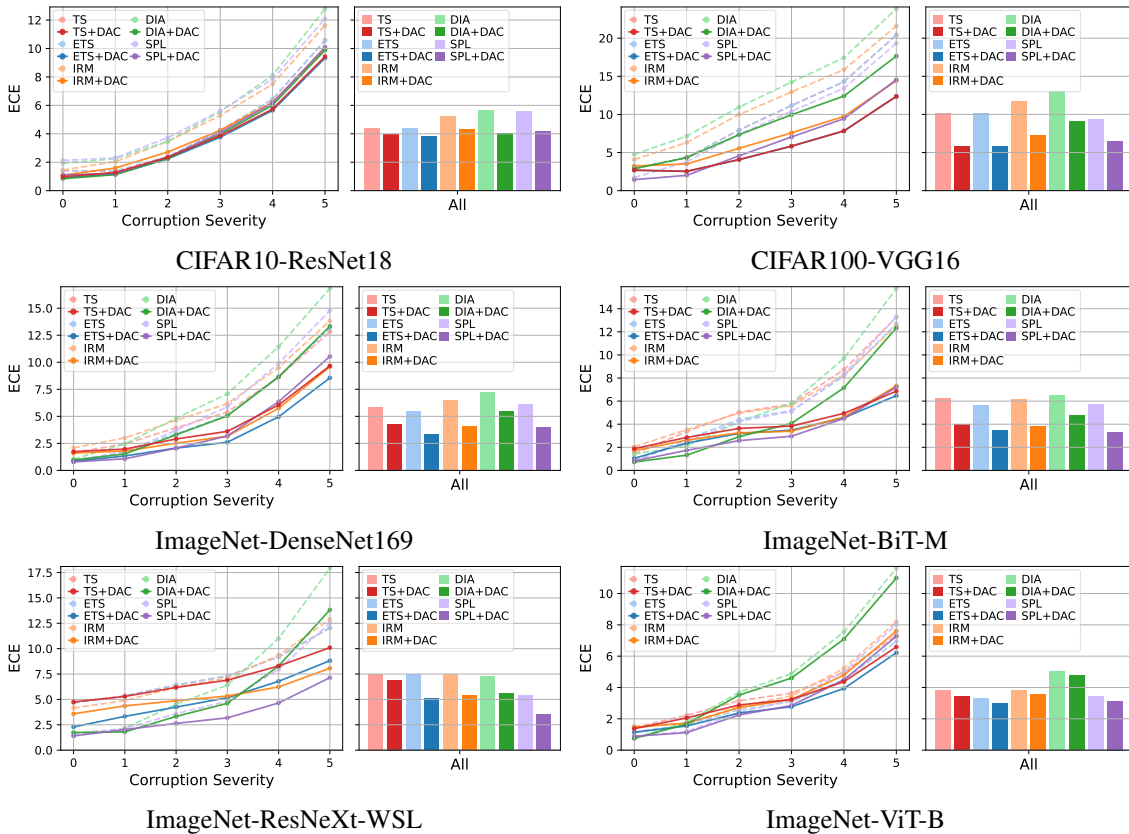


Figure 2: Expected calibration error ( $\times 10^2$ ) of post-hoc methods with and without our method DAC for different model and dataset combinations. **Line plots:** Macro-averaged ECE over all corruption types shown for each corruption severity, from in-domain to severity=5 (heavily corrupted). **Bar plots:** Macro-averaged ECE over all corruption types as well as across all severities. Our model captures domain-shift scenarios reliably and thus increases calibration (=decreases ECE) across the whole spectrum of corruptions.

as a layer importance analysis and a data efficiency analysis.

### 5.1 DAC Boosts Calibration Performance Beyond In-Domain Scenarios

We begin by systematically assessing whether the performance of state-of-the-art post-hoc calibration methods can be improved when extended by our proposed DAC method. In particular, we are interested in scenarios under domain-shift. To this end, we show calibration performance on CIFAR-C and ImageNet-C for severity levels from 1 to 5 and additionally provide results for in-domain scenarios (severity=0). Fig. 2 illustrates a comparison between stand-alone post-hoc methods and combined methods with DAC for various classifiers. The line charts reveal that DAC consistently improves the calibration performance of post-hoc methods in domain-shift cases. Tab. 2 underpins this performance increase even further by revealing a substantial decrease in the absolute ECE for heavily corrupted data (sever-

ity=5) scenarios when DAC is used. When optimizing for domain-shift performance, a sharp decline in in-domain performance is generally observed for other existing methods [37]. This is however not the case for our method, where we even observe slight improvements of in-domain ECE for many classifier and post-hoc method configurations, and for the few cases where in-domain ECE marginally increases (in the order of  $10^{-4}$  to  $10^{-3}$ ), the ECE in heavily corrupted scenarios decreases in the order of far more than a magnitude in comparison. Finally, in order to measure the overall improvement of DAC across the entire spectrum of corruptions from severity 0 to 5, we calculate the macro-averaged ECE over all corruption types and levels of severity for each method. We discover a consistent improvement for all post-hoc methods combined with DAC as opposed to stand-alone methods visualized in the bar charts in Fig. 2 and in Tab. 2. Moreover, Tab. 1 further reveals that DAC consistently boosts calibration performance across diverse architectures and datasets.

Since research regarding state-of-the-art post-hoc meth-

Table 2: Difference in expected calibration error ( $\times 10^2$ ) of post-hoc calibration methods with and without our method DAC. *IND*: In-domain, *SEV.5*: Heavily corrupted (severity of 5) and *ALL*: Macro-averaged ECE across all corruptions from severity=0 (in-domain) until severity=5 (heavily corrupted). For *ALL*, we additionally report the ratio to indicate overall performance gain. Post-hoc calibration methods combined with DAC consistently improve calibration in cases of heavy corruption as well as overall calibration (relative improvement of around 5-40%), while preserving in-domain performance (negative deltas are better).

	IND	SEV. 5	ALL	
TS	-0.42	-1.14	-0.46	10%
ETS	-0.49	-1.25	-0.56	13%
IRM	-0.36	-1.67	-0.92	18%
DIA	-1.09	-2.91	-1.67	29%
SPL	-1.02	-2.00	-1.45	26%

A.) CIFAR10 RESNET18

	IND	SEV. 5	ALL	
TS	-0.22	-8.05	-4.29	42%
ETS	-0.22	-8.06	-4.29	42%
IRM	-0.85	-7.15	-4.46	38%
DIA	-1.87	-6.20	-3.97	30%
SPL	-0.27	-4.77	-2.83	30%

B.) CIFAR100 VGG16

	IND	SEV. 5	ALL	
TS	+0.08	-3.16	-1.49	26%
ETS	+0.03	-4.61	-2.08	38%
IRM	-0.48	-4.25	-2.47	38%
DIA	-0.09	-3.49	-1.81	25%
SPL	-0.15	-4.23	-2.15	35%

C.) IMAGENET DENSENET169

	IND	SEV. 5	ALL	
TS	+0.47	-6.40	-2.26	36%
ETS	+0.28	-6.23	-2.13	38%
IRM	-0.34	-5.20	-2.34	38%
DIA	-0.69	-3.42	-1.75	27%
SPL	-0.01	-6.11	-2.41	42%

D.) IMAGENET BIT-M

	IND	SEV. 5	ALL	
TS	+0.09	-1.95	-0.58	8%
ETS	-2.37	-3.24	-2.39	32%
IRM	-0.57	-4.82	-2.02	27%
DIA	+0.30	-4.10	-1.64	23%
SPL	-0.25	-5.39	-1.94	36%

E.) IMAGENET RESNEXT-WSL

	IND	SEV. 5	ALL	
TS	-0.08	-0.74	-0.38	10%
ETS	-0.03	-0.72	-0.32	10%
IRM	-0.08	-0.59	-0.23	6%
DIA	-0.00	-0.62	-0.28	6%
SPL	+0.02	-0.74	-0.30	9%

F.) IMAGENET ViT-B

ods applied to recent large-scale neural networks is still lacking, we want to attempt to bridge this gap and show results for modern ResNet as well as transformer architectures trained on large corpuses of data. We make the same observation as Minderer et al. [24] that, in fact, even modern ResNet architectures are not well calibrated in domain-shift settings despite being pre-trained on huge amounts of data, yet transformer architectures perform particularly well. In our experiments, we observe that modern ResNet architectures (BiT-M and ResNeXt) can indeed be further calibrated with post-hoc methods. Especially, SPL+DAC performs best and reduces the ECE by around 37% for ResNeXt-WSL and 42% for BiT-M compared to the best-performing standard post-hoc method (Tab. 1). ViT-B on the other hand, can profit from existing post-hoc methods too, at least in-domain. For domain-shift scenarios, ViT outperforms all standard post-hoc methods, except when combined with DAC, in that case, ETS+DAC outperforms existing methods by 12%.

## 5.2 Calibration in OOD Scenarios

To complement the previous distributional shift experiments, we conduct additional experiments for the out-of-domain case, incorporating data samples with completely different classes w.r.t. the training data. Ideally, a well-calibrated uncertainty-aware model would produce high-confidence predictions for in-domain data and low-confidence ones for the OOD case, allowing for the detection of OOD data samples. Based on this idea, several metrics have been proposed in the OOD literature [13, 21, 20] to quantify the model performance in OOD scenarios, including FPR at 95% TPR, detection error, AUROC, AUPR-In/AUPR-Out, which we employ for our experiments.

To examine DAC in the OOD scenario, we set up the OOD dataset with in-domain data from ImageNet-1k and OOD data from ObjectNet-OOD (c.f. Section 4 for dataset descriptions). Top-class confidence predictions are produced by models trained and calibrated on ImageNet-1k with various calibration methods with and without the proposed DAC method. The OOD metrics are computed from the confidence predictions. We

summarize the results for the DenseNet169 backbone in Tab. 3.

Table 3: OOD performance with DenseNet169 trained on ImageNet-1k and using ImageNet-1k/ObjectNet-OOD as in-domain/OOD test sets, respectively. We observe that DAC consistently improves all the OOD metrics for all baseline methods.

	FPR @95% ↓	Det. Err ↓	AU- ROC ↑	AUPR- In ↑	AUPR- Out ↑
TS	21.47	22.86	84.92	81.14	86.87
+DAC	<b>20.73</b>	<b>22.30</b>	<b>85.50</b>	<b>81.86</b>	<b>87.46</b>
ETS	21.92	23.15	84.72	79.82	86.72
+DAC	<b>20.90</b>	<b>22.29</b>	<b>85.51</b>	<b>82.16</b>	<b>87.47</b>
IRM	21.51	22.31	83.62	81.22	86.10
+DAC	<b>4.87</b>	<b>20.72</b>	<b>85.81</b>	<b>82.73</b>	<b>87.90</b>
DIA	22.09	24.26	83.67	79.86	85.77
+DAC	<b>21.36</b>	<b>23.64</b>	<b>84.35</b>	<b>80.63</b>	<b>86.47</b>
SPL	21.66	24.38	83.65	79.95	85.78
+DAC	<b>20.89</b>	<b>22.30</b>	<b>85.54</b>	<b>82.05</b>	<b>87.56</b>

In general, we see that DAC yields more robust calibration in the OOD scenario, as demonstrated by its consistent improvement of OOD results.

### 5.3 Layer Importance for Calibration

Next, we want to investigate which layers of each classifier carry valuable information for DAC to yield calibrated predictions. For each layer, DAC learns a weight based on the importance of the respective layer (equation (7)). In Fig. 3 we demonstrate that DAC focuses on a few important layers, yet the logits layer is never one of them. This is particularly interesting because current state-of-the-art post-hoc calibration methods only focus on the logits vector for recalibration without even considering hidden layers of the classifier. Hence, we can conclude that one reason for DAC’s performance improvement can be attributed to its ability to take information from other layers into account apart from the logits layer.

Even though the layers DAC has access to are well distributed throughout the architecture of the classifier, we want to investigate whether DAC can capture all the necessary information present in all the layers of the classifier. To this end, we compare our simple and fast DAC method, which uses a subset of the layers, to a holistic DAC, which utilizes all layers. In Fig. 4 we illustrate the weights DAC assigns to each and every layer normalized to sum up to 1. The holistic DAC is able to attend to various layers; however, we observe that this does not necessarily result in better calibration performance, which can be attributed to overfitting.

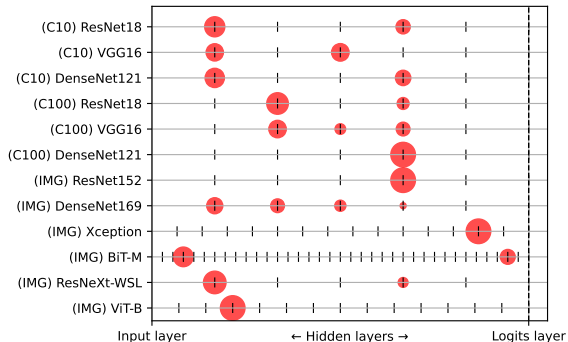


Figure 3: Importance of classifier layers found by DAC. The size of blobs indicates the magnitude of assigned weights for each layer after training of DAC from left (input) to right (logits).

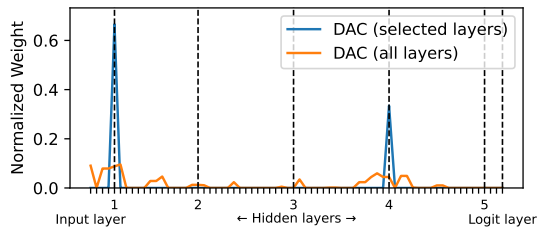


Figure 4: Comparison between our DAC with "selected layers" to a holistic DAC, which utilizes "all layers" present in ResNet18 trained on CIFAR10. DAC is able to capture the most relevant areas in layer space with important information for calibration.

### 5.4 Data Efficiency of DAC

Lastly, we investigate how sensitive our method is to various sample sizes of the validation set, which is the data set to train post-hoc models. In particular, we want to understand, how calibration performance behaves when the validation set is small. We focus on the best-performing methods, namely ETS+DAC and SPL+DAC, and compare them to the respective stand-alone methods, ETS and SPL. Additionally, we incorporate TS in our study, since this method is least likely to suffer from overfitting because it comprises of only one parameter to train. We encounter in Fig. 5 that no matter which validation set size we use, combinations with DAC perform better than without DAC. Additionally, DAC does not overfit the data for small validation set sizes.



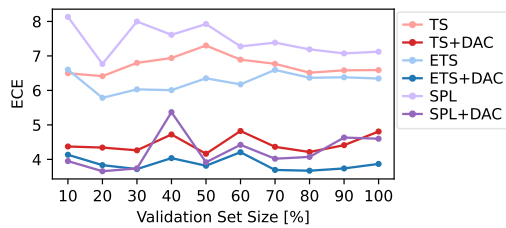


Figure 5: DAC is robust across different validation set sizes (10% - 100%) for DenseNet169 trained on ImageNet ( $ECE (\times 10^2)$ ).

## 6 Conclusion

In this work, we have introduced an accuracy-preserving density-aware calibration method that can readily be applied with SOTA post-hoc methods in order to boost domain-shift and OOD calibration performance. We found that our proposed method DAC in combination with existing post-hoc calibration methods yields robust predictive uncertainty estimates for any level of domain-shift, from in-domain to truly OOD scenarios. In particular, ETS+DAC as well as SPL+DAC performed the best. We further demonstrated that hidden layers in classifiers carry valuable information for accurately predicting uncertainty estimates. Lastly, we show that even for recently developed large-scale models pre-trained on vast amounts of data can be calibrated effectively, opening up new research directions within the field of post-hoc calibration for entirely new applications.

## References

- [1] A. Ashukha, A. Lyzhov, D. Molchanov, D. Vetrov, Pitfalls of in-domain uncertainty estimation and ensembling in deep learning, arXiv preprint arXiv:2002.06470.
- [2] A. Barbu, D. Mayo, J. Alverio, W. Luo, C. Wang, D. Gutfreund, J. Tenenbaum, B. Katz, Objectnet: A large-scale bias-controlled dataset for pushing the limits of object recognition models, *Advances in neural information processing systems* 32.
- [3] F. Chollet, Xception: Deep learning with depth-wise separable convolutions, in: *Proceedings of the IEEE conference on computer vision and pattern recognition*, 2017, pp. 1251–1258.
- [4] J. Deng, W. Dong, R. Socher, L.-J. Li, K. Li, L. Fei-Fei, Imagenet: A large-scale hierarchical image database, in: *2009 IEEE conference on computer vision and pattern recognition*, Ieee, 2009, pp. 248–255.
- [5] A. Dosovitskiy, L. Beyer, A. Kolesnikov, D. Weissenborn, X. Zhai, T. Unterthiner, M. Dehghani, M. Minderer, G. Heigold, S. Gelly, et al., An image is worth 16x16 words: Transformers for image recognition at scale, arXiv preprint arXiv:2010.11929.
- [6] A. Dosovitskiy, L. Beyer, A. Kolesnikov, D. Weissenborn, X. Zhai, T. Unterthiner, M. Dehghani, M. Minderer, G. Heigold, S. Gelly, et al., An image is worth 16x16 words: Transformers for image recognition at scale, arXiv preprint arXiv:2010.11929.
- [7] Y. Gal, Z. Ghahramani, Dropout as a bayesian approximation: Representing model uncertainty in deep learning, in: *international conference on machine learning*, 2016, pp. 1050–1059.
- [8] C. Guo, G. Pleiss, Y. Sun, K. Q. Weinberger, On calibration of modern neural networks, in: *Proceedings of the 34th International Conference on Machine Learning-Volume 70*, JMLR. org, 2017, pp. 1321–1330.
- [9] K. Gupta, A. Rahimi, T. Ajanthan, T. Mensink, C. Sminchisescu, R. Hartley, Calibration of neural networks using splines, in: *International Conference on Learning Representations*, 2021. URL <https://openreview.net/forum?id=eQe8DEWNN2W>
- [10] K. He, X. Zhang, S. Ren, J. Sun, Deep residual learning for image recognition, in: *Proceedings of the IEEE conference on computer vision and pattern recognition*, 2016, pp. 770–778.
- [11] K. He, X. Zhang, S. Ren, J. Sun, Identity mappings in deep residual networks, in: *European conference on computer vision*, Springer, 2016, pp. 630–645.
- [12] D. Hendrycks, T. Dietterich, Benchmarking neural network robustness to common corruptions and perturbations, *International Conference on Learning Representations* 2019.
- [13] D. Hendrycks, K. Gimpel, A baseline for detecting misclassified and out-of-distribution examples in neural networks, in: *ICLR*, 2017.
- [14] D. Hendrycks, M. Mazeika, S. Kadavath, D. Song, Using self-supervised learning can improve model robustness and uncertainty, *Advances in neural information processing systems* 32.

- [15] G. Huang, Z. Liu, L. Van Der Maaten, K. Q. Weinberger, Densely connected convolutional networks, in: Proceedings of the IEEE conference on computer vision and pattern recognition, 2017, pp. 4700–4708.
- [16] A. Kolesnikov, L. Beyer, X. Zhai, J. Puigcerver, J. Yung, S. Gelly, N. Houlsby, Big transfer (bit): General visual representation learning, in: European conference on computer vision, Springer, 2020, pp. 491–507.
- [17] A. Krizhevsky, G. Hinton, et al., Learning multiple layers of features from tiny images.
- [18] M. Kull, M. Perello Nieto, M. Kängsepp, T. Silva Filho, H. Song, P. Flach, Beyond temperature scaling: Obtaining well-calibrated multi-class probabilities with dirichlet calibration, *Advances in neural information processing systems* 32.
- [19] B. Lakshminarayanan, A. Pritzel, C. Blundell, Simple and scalable predictive uncertainty estimation using deep ensembles, *Advances in neural information processing systems* 30.
- [20] K. Lee, K. Lee, H. Lee, J. Shin, A simple unified framework for detecting out-of-distribution samples and adversarial attacks, in: *NeurIPS*, 2018.
- [21] S. Liang, Y. Li, R. Srikant, Enhancing the reliability of out-of-distribution image detection in neural networks, in: *ICLR*, 2018.
- [22] D. K. Mahajan, R. B. Girshick, V. Ramanathan, K. He, M. Paluri, Y. Li, A. Bharambe, L. van der Maaten, Exploring the limits of weakly supervised pretraining, in: *ECCV*, 2018.
- [23] D. Milius, R. Camoriano, P. Michiardi, L. Rosasco, M. Filippone, Dirichlet-based gaussian processes for large-scale calibrated classification, *Advances in Neural Information Processing Systems* 31.
- [24] M. Minderer, J. Djolonga, R. Romijnders, F. Hubis, X. Zhai, N. Houlsby, D. Tran, M. Lucic, Revisiting the calibration of modern neural networks, *Advances in Neural Information Processing Systems* 34 (2021) 15682–15694.
- [25] R. Müller, S. Kornblith, G. E. Hinton, When does label smoothing help?, *Advances in neural information processing systems* 32.
- [26] M. P. Naeini, G. Cooper, M. Hauskrecht, Obtaining well calibrated probabilities using bayesian binning, in: *Twenty-Ninth AAAI Conference on Artificial Intelligence*, 2015.
- [27] Y. Ovadia, E. Fertig, J. Ren, Z. Nado, D. Sculley, S. Nowozin, J. Dillon, B. Lakshminarayanan, J. Snoek, Can you trust your model’s uncertainty? evaluating predictive uncertainty under dataset shift, in: *Advances in Neural Information Processing Systems*, 2019, pp. 13991–14002.
- [28] J. C. Platt, Probabilistic outputs for support vector machines and comparisons to regularized likelihood methods, in: *Advances in large margin classifiers*, MIT Press, 1999, pp. 61–74.
- [29] A. Rahimi, K. Gupta, T. Ajanthan, T. Mensink, C. Sminchisescu, R. Hartley, Post-hoc calibration of neural networks, *arXiv preprint arXiv:2006.12807*.
- [30] A. Rahimi, A. Shaban, C.-A. Cheng, R. Hartley, B. Boots, Intra order-preserving functions for calibration of multi-class neural networks, *Advances in Neural Information Processing Systems* 33 (2020) 13456–13467.
- [31] M. Sensoy, L. Kaplan, M. Kandemir, Evidential deep learning to quantify classification uncertainty, in: *Advances in Neural Information Processing Systems*, 2018, pp. 3179–3189.
- [32] K. Simonyan, A. Zisserman, Very deep convolutional networks for large-scale image recognition, *arXiv preprint arXiv:1409.1556*.
- [33] Y. Sun, Y. Ming, X. Zhu, Y. Li, Out-of-distribution detection with deep nearest neighbors, *arXiv preprint arXiv:2204.06507*.
- [34] S. Thulasidasan, G. Chennupati, J. A. Bilmes, T. Bhattacharya, S. Michalak, On mixup training: Improved calibration and predictive uncertainty for deep neural networks, *Advances in Neural Information Processing Systems* 32.
- [35] C. Tomani, F. Buettner, Towards trustworthy predictions from deep neural networks with fast adversarial calibration, in: *Thirty-Fifth AAAI Conference on Artificial Intelligence*, 2021.
- [36] C. Tomani, D. Cremers, F. Buettner, Parameterized temperature scaling for boosting the expressive power in post-hoc uncertainty calibration, in: *European Conference on Computer Vision*, Springer, 2022, pp. 555–569.
- [37] C. Tomani, S. Gruber, M. E. Erdem, D. Cremers, F. Buettner, Post-hoc uncertainty calibration for domain drift scenarios, in: *Proceedings of the IEEE/CVF Conference on Computer Vision and Pattern Recognition*, 2021, pp. 10124–10132.

- [38] Y. Wald, A. Feder, D. Greenfeld, U. Shalit, On calibration and out-of-domain generalization, *Advances in neural information processing systems* 34 (2021) 2215–2227.
- [39] D.-B. Wang, L. Feng, M.-L. Zhang, Rethinking calibration of deep neural networks: Do not be afraid of overconfidence, *Advances in Neural Information Processing Systems* 34 (2021) 11809–11820.
- [40] Y. Wen, P. Vicol, J. Ba, D. Tran, R. Grosse, Flipout: Efficient pseudo-independent weight perturbations on mini-batches, *arXiv preprint arXiv:1803.04386*.
- [41] J. Wenger, H. Kjellström, R. Triebel, Non-parametric calibration for classification, in: *International Conference on Artificial Intelligence and Statistics*, PMLR, 2020, pp. 178–190.
- [42] S. Xie, R. Girshick, P. Dollár, Z. Tu, K. He, Aggregated residual transformations for deep neural networks, in: *Proceedings of the IEEE conference on computer vision and pattern recognition*, 2017, pp. 1492–1500.
- [43] Y. Yu, S. Bates, Y. Ma, M. I. Jordan, Robust calibration with multi-domain temperature scaling, *arXiv preprint arXiv:2206.02757*.
- [44] B. Zadrozny, C. Elkan, Obtaining calibrated probability estimates from decision trees and naive bayesian classifiers, in: *Icml*, Vol. 1, Citeseer, 2001, pp. 609–616.
- [45] B. Zadrozny, C. Elkan, Transforming classifier scores into accurate multiclass probability estimates, in: *Proceedings of the eighth ACM SIGKDD international conference on Knowledge discovery and data mining*, 2002, pp. 694–699.
- [46] H. Zhang, M. Cisse, Y. N. Dauphin, D. Lopez-Paz, mixup: Beyond empirical risk minimization, *arXiv preprint arXiv:1710.09412*.
- [47] J. Zhang, B. Kailkhura, T. Han, Mix-n-match: Ensemble and compositional methods for uncertainty calibration in deep learning, in: *International Conference on Machine Learning (ICML)*, 2020.